Available online at www.sciencedirect.com
ScienceDirect
International Journal of Heat and Mass Transfer 50 (2007) 1302–1313
International Journal of HEAT and MASS TRANSFER
www.elsevier.com/locate/ijhmt

Analytical and experimental study of premixed methane–air flame propagation in narrow channels

C.Y.H. Chao [a,*], K.S. Hui [a], W. Kong [a], P. Cheng [b], J.H. Wang [a]

[a] Department of Mechanical Engineering, The Hong Kong University of Science and Technology, Clear Water Bay, Kowloon, Hong Kong, China
[b] School of Mechanical and Power Engineering, Shanghai Jiaotong University, Shanghai 200030, PR China

Received 15 May 2006; received in revised form 19 September 2006
Available online 13 November 2006

Abstract

This study investigates analytically and experimentally the influence of preheat temperature on flame propagation and extinction of premixed methane–air flame in single quartz tubes with inner tube diameters of 3.9, 3, 2 and 1 mm respectively. The effects of preheat temperature, tube diameter, equivalence ratio and mixture flow rate on the flame speed and extinction conditions are determined. The analytical results show that high preheat temperature of the mixture can effectively suppress flame quenching, and the occurrence of stable solution in the slow flame branch extends the flammability limit leading to possible flame propagation in mini channels. Experimental results confirm that the flame speed increases and the flammability limit shifts toward the fuel lean direction either through increasing the preheat temperature or decreasing the mixture flow rate, or both. Decrease of propagating flame speed is observed before the stoichiometric equivalence ratio at high preheat temperatures. The analytical model provides insights into how propagating flame in mini channels can be sustained; however, the model is only good at predicting flame speed near the fuel lean branch. Influence of Cu^{2+} ions exchanged zeolite 13X catalyst on flame speed is also addressed. It is noted that the zeolite based catalyst can lower the preheat temperature requirement in order to sustain the flame propagation in narrow channels.

Keywords: Narrow channels; Flammability limits; Flame speed; Activation energy; Asymptotic analysis

1. Introduction

Depending on the battery assessment technique, energy densities of hydrocarbon fuels can be 12–100 times higher than those of advanced electrochemical batteries. Therefore, a great deal of attention has recently been focused on the development and application of MEMS devices to generate power through combustion of hydrocarbon fuels [1]. Various kinds of power devices have been developed rapidly, such as micro-gas turbine engines [2], Wankel rotary internal combustion engines [3], free-piston knock engine [4], Swiss roll combustor [5], thermoelectrics system [6] and thermophotovoltaic system [7]. These previous studies emphasized mainly on the fabrication processes and the performance of the devices [2–7].

For the design of power-MEMS devices, mini combustion characteristics are important aspects that need careful consideration. As devices are scaled down, their surface area to volume ratio becomes larger, resulting in larger heat loss rate relative to heat generation rate. This can cause flame quenching. Therefore, it is very important to understand the fundamental combustion characteristics including flame propagation and extinction in mini channels [3,8–14]. Zamashchikov [10] studied flame propagation in propane–air and hydrogen–air mixtures flowing in a horizontal quartz tube of inner diameter of 2.7 mm at temperature of 18–23 °C and atmospheric pressure. It was found that basic characteristics of a combustion wave propagating in a tube depend strongly on the kind of fuel. In another paper, Zamashchikov [11] investigated the

* Corresponding author. Tel.: +852 2358 7210; fax: +852 2358 1543.
E-mail address: meyhchao@ust.hk (C.Y.H. Chao).

0017-9310/$ - see front matter © 2006 Elsevier Ltd. All rights reserved.
doi:10.1016/j.ijheatmasstransfer.2006.09.012

Nomenclature

B	Arrhenius pre-exponential factor [s^{-1}]
c_p	heat capacity for gas [kJ/(kg K)]
D	molecular diffusion coefficient [m^2/s]
E	activation energy [J/mol]
h_i	dimensional heat transfer coefficient on the inner wall surface [W/(m^2 K)]
H_i	non-dimensional heat transfer rate on the inner wall surface, $\frac{h_i \varepsilon \beta}{\rho c_p S_L}$
h_o	dimensional heat transfer coefficient on the outer wall surface [W/(m^2 K)]
H_o	non-dimensional heat transfer rate on the outer wall surface, $\frac{h_o \varepsilon \beta}{\rho c_p S_L}$
k	thermal conductivity for gas [W/(m K)]
k_w	thermal conductivity for wall [W/(m K)]
K	non-dimensional parameter, $\frac{k_w}{k}\frac{\tau}{R}$
Le	Lewis number, α/D, dimensionless
Q	reaction heat release per unit mass of fuel [kJ/kg]
R	dimensional radius of the tube [m]
Ru	universal gas constant [kJ/(kmol K)]
S_L	asymptotic value of the adiabatic planar burning velocity calculated in the limit $\beta \gg 1$, $S_L = \sqrt{2\beta^{-2} B \alpha Le \exp(-T_a/2T_{ad})}$ [m/s]
T_0	initial tube wall temperature [K]
T	local temperature [K]
T_a	the activation temperature, E/Ru [K]
T_{ad}	adiabatic flame temperature, $T_0 + QY_{F0}/c_p$ [K]
u'_f	dimensional flame speed relative to the tube wall [m/s]
u'_0	dimensional flow velocity relative to the wall [m/s]
u'	relative flame speed, $u'_0 - u'_f$ [m/s]
U_f	non-dimensional flame speed relative to the tube wall, u'_f/S_L
U_0	non-dimensional flow velocity relative to the wall, u'_0/S_L
U	normalized flame speed, $U_0 - U_f$, dimensionless
x'	dimensional longitudinal coordinate [m]
x	non-dimensional longitudinal coordinate, x'/δ_T
Y_F	mass fraction of fuel, dimensionless
Y_{F0}	mass fraction of fuel in fresh mixture, dimensionless
Y	normalized mass fraction, Y_F/Y_{F0}, dimensionless

Greek symbols

α	thermal diffusivity for gas, $k/\rho c_p$ [m^2/s]
α_w	thermal diffusivity for wall, $k_w/\rho_w c_w$ [m^2/s]
β	Zeldovich number $T_a(T_{ad} - T_0)/T_{ad}^2$, dimensionless
δ_T	thickness of laminar flame, α/S_L [m]
ε	ratio of δ_T to R denoted by δ_T/R, dimensionless
γ	heat release parameter, $(T_{ad} - T_0)/T_{ad}$, dimensionless
λ	eigenvalues
θ	non-dimensional temperature, $(T - T_0)/(T_{ad} - T_0)$
ρ	density for gas [kg/m^3]
ρ_w	density for wall [kg/m^3]
τ	dimensional wall thickness [m]
ω'	reaction rate, $\rho B Y_F \exp(-T_a/T)$ [kg/m^3 s]
ω	non-dimensional reaction rate, $\frac{\beta^2}{2Le} Y \exp\left\{\frac{\beta(\theta-1)}{1+\gamma(\theta-1)}\right\}$

Subscript

w	the wall

dependence of the flame-front curvature on the composition of the propane–air mixture in a horizontal quartz tube of inner diameters of 3.2, 5.1 and 7 mm at temperature of 18–23 °C and atmospheric pressure. It was found that the shape of the symmetric flame-front in mini tube was most probably determined by heat transfer between the flame and the tube walls. The range of flame existence in terms of the composition of the mixture became narrower with decreasing tube diameter. As the tube diameter decreased, the peak flame velocity was shifted to the region of rich mixtures. Apart from the conventional fast flame speed regime, the existence of slow flame speed regime was experimentally and theoretically investigated by Zamashchikov and Minaev [8,9]. The existence of slow flame speed regime was based on preheating unburnt mixture through the wall of the tube by the burnt mixture. Later, Ju and Xu [12] investigated analytically, experimentally, and numerically the flame propagation and extinction of premixed propane–air flame in mini tube at room temperature and atmospheric pressure. Experiments were conducted in a tube with inner diameter of 5 mm and 600 mm long. The analytical model is based on preheating unburnt mixture through wall of the tube by the flame at room temperature. The analytical solution for normalized flame speed is expressed in terms of material properties of the tube, normalized rate of heat transfer on the inner wall surface and Zeldovich number β. These studies [8,9,12] show that the wall-flame interaction via heat recirculation leads to multiple flame regimes and extinction limits. The existence of the slow flame regime extends the flammability limit and renders the classical quenching diameter inapplicable.

It should be noted that the dimension of inner diameter of the tubes used by Zamashchikov [8,10,11] and Ju and Xu [12] were larger than the quenching distance of the corresponding fuels at their experimental conditions. The quenching distance is defined as the smallest diameter of the tube which prevents flame propagation [15]. The quenching distance in a channel is about 15 times of the

flame thickness [16–18]. Previous studies [3,15,19] show that quenching distance is dependent on initial temperature of the mixture and the wall temperature of the combustor. The increase of initial temperature of the mixture and the wall of combustor will decrease the quenching distance. In order to study the combustion characteristics in mini tubes with inner diameters smaller than the conventional quenching distance of the employed mixture measured at room temperature, preheating of the tubes can be one effective way. Fu et al. [3] studied premixed methane–air flame (equivalence ratio = 1.1) in a vertical quartz tube of inner diameters of 0.9–5 mm at temperature of 20–907 °C and atmospheric pressure. It was found that sustained combustion in channels smaller than the quenching distance is possible through reducing heat losses by preheating the unburnt mixture with electrical heater or recirculating exhaust gases around the exterior of the bundled tubes. Maruta et al. [13] studied premixed methane–air flame (equivalence ratio = 0.85) in a horizontal quartz tube of inner diameter of 2 mm at a temperature of 857–1047 °C and atmospheric pressure. Characteristics of combustion in a heated mini channel with a temperature gradient were investigated experimentally, analytically, and numerically. One-dimensional stability analysis and computation with detailed chemistry were made to obtain an overview of the flame stability and to examine the structures of those flames in detail. Maruta et al. [14] also studied effects of the equivalence ratio and the volume flow rate of methane–air mixture on the characteristics of combustion in a horizontal and a U-shaped quartz tube of inner diameter of 2 mm at a temperature of 1000 °C and atmospheric pressure. It was found that combustion can be successfully attained even for methane–air mixtures with equivalence ratios outside the conventional flammability limits. These studies [3,13,14] show that initial preheat temperature is an important factor for sustainable combustion in mini tubes although not much work has been devoted to the study of this effect.

Although sustainable combustion in very narrow tubes (0.9–2 mm) can be achieved through a very high preheat temperature (~1000 °C), it is not feasible for the development of micro-scale power devices. A potential means of reducing the impact of heat losses is to employ catalytic combustion. Catalyst has been used to reduce the activation energy for the reaction allowing the process to maintain a fast rate, where the self-sustaining reaction may occur at lower temperatures [20]. In addition, catalytic combustion can also be carried out in lean fuel where the reaction temperature is reduced, thus a lower concentration of NO_x pollutants can be achieved [21]. Rudham and Sanders [22] studied the oxidation of methane catalyzed by zeolite 13X in a flow system with reaction temperature between 253 and 563 °C. It was found that kinetics of methane oxidation by transition metal ions exchanged zeolite 13X was faster than the corresponding bulk oxides. Nekrasov et al. [23] also show that zeolite based catalyst (CuZSM-5) exhibits higher activity in methane oxidation than Cu–SiO_2 catalyst. Although transition metals based zeolite can be a good choice as a cheap catalyst with easy preparation process for combustion-based micro-combustors, there has been very little study about them.

Our preliminary experiments showed that flame cannot be sustained and propagated in narrow tubes (having diameters smaller than the quenching distance of the corresponding fuel at room temperature) through preheating unburnt mixture by the mechanism of flame-wall interaction at room temperature. Therefore, the present study aims to investigate the influence of preheat temperature on flame propagation and extinction feature of premixed methane–air flame in mini tubes. At first, activation energy asymptotics (AEA) is used to obtain an analytical expression for the dimensionless flame speed, dimensionless activation energy (Zeldovich number β) and dimensionless heat transfer coefficient in the mini tube. It is shown that β is one of the important parameters to sustain combustion in mini tubes, which was not investigated thoroughly in previous works. Physical insights into the sustainability of combustion in small-scale or microchannels are obtained from the analytical model which can be used to assist in the design of micro-power devices or micro-reactors. The effects of the tube diameter, equivalence ratio, mixture flow velocity, and preheat temperature on combustion characteristics in the mini channel are studied experimentally so as to compare with the analytical results. Influence of Cu^{2+} ions exchanged zeolite 13X catalyst (Cu-13X) on characteristics of combustion of methane–air flame in mini channel is also addressed.

2. Analytical model

The formulation of the model is similar to Ju and Xu [12] and more detailed elaboration is given in this work. The major difference of the present model with Ju and Xu's model is the selection of the inner wall and the outer wall heat transfer coefficients h_i and h_o which are of the order of $O(\beta^{-1})$. This choice is based on previous asymptotic study of non-adiabatic combustion problem which showed that extinction occurs for $O(\beta^{-1})$ values of the volumetric heat-loss coefficient [17]. When the uniformly premixed gas mixture flows through a tube, a pilot flame is used to ignite the mixture at the exit of the tube. If the flame speed is greater than the mixture flow velocity, the flame will propagate inside the tube. The flame propagation in a macro-tube is usually two-dimensional in nature. However, in mini tubes where the tube diameter and the tube wall thickness are much smaller than the tube length, the problem can be simplified as one-dimension [24]. Thus, one-dimensional equations will be used to analyze the micro-combustion characteristics in this paper.

We now analyze the influence of preheat temperature on combustion characteristics in mini channels, where temperature of the initial fresh mixture and the initial wall temperature are raised by an external heat source to T_0. In this analysis, x' denotes the longitudinal coordinate along the

axis, and R denotes the radius of the tube. The flames propagate along the x' direction with speed $-u'_f$ relative to the tube wall. Thermal-diffusive approximation with constant density ρ, thermal diffusivity α, heat capacity c_p and diffusion coefficient D are adopted in this analysis. The mixture flow is unaffected by the combustion process and the flow velocity along the positive x' direction relative to the wall is denoted by u'_0. It is assumed that the fuel is completely consumed in the flame. Under this situation, it is reasonable to expect the air fuel mixture to act like a single reactant that fuses into a product. Thus the one-step irreversible reaction of the form $F \to P + Q$ can be adopted [17] where F denotes the fuel/oxidant, P the products and Q the reaction heat release per unit of fuel. The combustion rate ω', defined as the mass of fuel consumed per unit volume and unit time, is given by an Arrhenius law of the form

$$\omega' = \rho B Y_F \exp(-T_a/T) \tag{1}$$

where B, Y_F, T, and T_a represent, respectively, the pre-exponential factor, the mass fraction of fuel, the local temperature of the mixture, and the activation temperature with $T_a = E/Ru$ where E and Ru are the activation energy and the universal gas constant.

To formulate the problem in a dimensionless form, laminar flame velocity is normalized by $S_L = \sqrt{2\beta^{-2} B\alpha Le \exp(-T_a/2T_{ad})}$, which is the asymptotic value of the adiabatic planar burning speed calculated in the limit of $\beta \gg 1$ [25]. Here $T_{ad} = T_0 + QY_{F0}/c_p$ is the adiabatic flame temperature; Y_{F0} is the mass fraction of fuel in the fresh mixture; $\beta = T_a(T_{ad} - T_0)/T_{ad}^2$ is the Zeldovich number and $Le = \alpha/D$ is the Lewis number. The corresponding thickness of the laminar flame is of the order of $\delta_T = \alpha/S_L$. For a non-dimensional description, δ_T is used to normalize the longitudinal coordinates $x = x'/\delta_T$. The ratio of δ_T to R is a dimensionless parameter denoted by $\varepsilon = \delta_T/R$. A micro-channel corresponds to the limit of large ε. The ratio $Y = Y_F/Y_{F0}$ is the dimensionless mass fraction and $\theta = (T - T_0)/(T_{ad} - T_0)$ is the dimensionless temperature. By setting the coordinate on the moving flame front, the dimensionless governing equations (with radiation, pressure diffusion and external forces neglected) for the gas and wall are

$$U\frac{d\theta}{dx} = \frac{d^2\theta}{dx^2} - \frac{H_i}{\beta}(\theta - \theta_w) + \omega \tag{2}$$

$$U\frac{dY}{dx} = \frac{1}{Le}\frac{d^2Y}{dx^2} - \omega \tag{3}$$

$$K\frac{d^2\theta_w}{dx^2} + \frac{\alpha}{\alpha_w}KU_f\frac{d\theta_w}{dx} + \frac{H_i}{\beta}(\theta - \theta_w) - \frac{H_o\theta_w}{\beta} = 0 \tag{4}$$

In small/micro-scale combustion, coupling between the flame and the wall is important. Eq. (4) describes the coupling between the gas and the solid (tube wall). In Eq. (4), for the wall, the governing heat transfer modes are heat conduction (the first term), enthalpy transport or convection term (the second term), inner (the third term) and outer (the fourth term) wall surface heat convection. $U_o = u'_o/S_L$, $U_f = u'_f/S_L$ and $U = U_0 - U_f$. The reaction heat release term Q was embedded in dimensionless reaction rate $\omega = \frac{\beta^2}{2Le} Y \exp\left\{\frac{\beta(\theta-1)}{1+\gamma(\theta-1)}\right\}$ where $\gamma = (T_{ad} - T_0)/T_{ad}$ is the heat release parameter. $K = \frac{k_w}{k}\frac{\tau}{R}$, where k is the thermal conductivity, the subscript w denotes the wall and τ is the wall thickness. The dimensionless heat transfer coefficients are $H_i = \frac{h_i \varepsilon \beta}{\rho c_p S_L}$ and $H_o = \frac{h_o \varepsilon \beta}{\rho c_p S_L}$, respectively, where h_i is the heat transfer coefficient on the inner wall surface which is related to the flame-wall interaction; h_o is the heat transfer coefficient on the outer wall surface which is related to the wall heat loss to the ambient air while the outside surface of the wall is cooled down by natural convection and radiation.

The boundary conditions are

$$x \to -\infty, \quad \theta = \theta_w = 0, \quad Y = 1, \quad x \to +\infty,$$
$$\frac{d\theta}{dx} = \frac{d\theta_w}{dx} = 0, \quad Y = 0 \tag{5}$$

In the presence of heat loss, the dimensionless wall temperature far in the downstream direction in the burned gas must go to zero. There is a cooling region in the burned gas that extends to a distance of $x \sim O(\beta)$. Thus the far-field temperature in the burned gas can be analyzed as follows. Let $\xi = \beta^{-1}x$ and introduce the following general forms of outer expansions based on Taylor series expansion:

$$\theta(\xi) = \theta^0(\xi) + \theta^1(\xi)/\beta + \cdots,$$
$$\theta_w(\xi) = \theta_w^0(\xi) + \theta_w^1(\xi)/\beta + \cdots \tag{6}$$

The governing equations for θ^0 and θ_w^0 can be rewritten as

$$U\frac{d\theta^0}{d\xi} = -H_i(\theta^0 - \theta_w^0) \tag{7}$$

$$H_i(\theta^0 - \theta_w^0) - H_o\theta_w^0 = 0 \tag{8}$$

The solution that decays as $\xi \to \infty$ for θ^0 and θ_w^0 are

$$\theta^0(\xi) = \theta_f^0 \exp\left(-\frac{H_iH_o}{U(H_i + H_o)}\xi\right) \tag{9}$$

$$\theta_w^0(\xi) = \frac{H_i}{H_i + H_o}\theta_f^0 \exp\left(-\frac{H_iH_o}{U(H_i + H_o)}\xi\right) \tag{10}$$

In the preheat zone, the governing equation for the temperature in the leading order becomes

$$U\frac{d\theta^0}{dx} = \frac{d^2\theta^0}{dx^2} \tag{11}$$

The solution that decays as $x \to -\infty$ is

$$\theta^0(x) = \theta_f^0 \exp(Ux) \quad \text{and} \quad \theta_w^0 = \frac{H_i}{H_i + H_o}\theta_f^0 \tag{12}$$

The preheat zone is dominated by the convection–diffusion effects. After the reaction sheet, it is the convection-heat loss dominated zone. In the large activation energy limit, using the boundary condition, the fuel concentration in zeroth order can be obtained as

$$Y^0 = \begin{cases} 1 - \exp(LeUx), & x < 0 \\ 0, & x > 0 \end{cases} \tag{13}$$

In order to complete the analysis, the general forms of inner expansions based on the Taylor series expansion are used in the thin reaction zone in the form

$$\theta(\eta) = \Theta^0(\eta) + \Theta^1(\eta)/\beta + \Theta^2(\eta)/\beta^2 + \cdots,$$
$$Y(\eta) = y^1(\eta)/\beta + y^2(\eta)/\beta^2 + \cdots \tag{14}$$

where η is the stretched coordinate given by $\eta = \beta x$. To leading order $\frac{d^2\Theta^0}{d\eta^2} = 0$, the solution needs to be continuous and smooth across the reaction sheet and tends to constant as $\eta \to \pm\infty$. To the next order, the equations are

$$\frac{d^2\Theta^1}{d\eta^2} + \beta^{-1}\omega = 0 \tag{15}$$

$$\frac{1}{Le}\frac{d^2y^1}{d\eta^2} - \beta^{-1}\omega = 0 \tag{16}$$

Adding (15) and (16), integrating, and using the matching conditions for $\eta \to +\infty$ provides a relation between the temperature and concentration gradients valid throughout the reaction zone,

$$\frac{d\Theta^1}{d\eta} + \frac{1}{Le}\frac{dy^1}{d\eta} = 0 \tag{17}$$

and the jump condition is

$$\left[\frac{d\theta^0}{dx} + \frac{1}{Le}\frac{dY^0}{dx}\right]_-^+ = 0 \tag{18}$$

Thus the flame temperature is given by

$$\theta_f^0 = \frac{\beta U^2(H_i + H_o)}{H_i H_o + \beta U^2(H_i + H_o)} \tag{19}$$

Integrating (17) and using the result to substitute for y^1 in (16), multiply by $d\Theta^1/dx$ and integrate across the reaction zone, the jump condition is obtained as

$$\left[\frac{d\Theta^1}{d\eta}\right]_-^+ = -\left[\frac{1}{Le}\frac{dy^1}{d\eta}\right]_-^+ = -\exp\left[\beta(\theta_f - 1)/2\right] \tag{20}$$

Directly using Eq. (13) to Eq. (20), the normalized flame speed can be obtained as

$$\ln U^2 = -\frac{\beta H_i H_o}{H_i H_o + \beta U^2(H_i + H_o)} \tag{21}$$

which shows that U is a function of H_i/β and H_i/H_o.

3. Experimental

3.1. Setup for study of combustion of methane–air flame in mini-channels

According to the conditions used in the theoretical analysis, experiments are designed to investigate the influence of preheat temperature on flame speed at various tube radius, volume flow rates and equivalence ratio. The fuel lean region is studied since it is more reasonable to operate premixed-type mini-combustors in this region due to fuel economy and the reduction of pollutant generation. The theoretical conditions are tried to be matched with the experimental conditions but it is difficult in maintaining constant preheat temperature all over the system at those high temperature cases for mini channels. This may affect how close the experimental data fit with the theoretical predictions.

Experiments were conducted using the premixed methane–air mixture burning in a horizontal quartz tube whose wall was cooled under natural convection at room temperature and atmospheric pressure. The methodology used in this study is similar to those of Zamashchikov [11] and Maruta et al. [13]. The experimental apparatus consisted of a pressurized gas cylinder (methane) with two (coarse and fine) pressure regulators, a compressed air system with filter, two digital mass flow controllers (AALBORG, Model DFC26, methane (0–10 ml/min), air (0–50 ml/min), accuracy: ±1% FS), a mixer, pressure gauges (Cecomp Electronics, range: 0–15 psi, accuracy: ±0.25% FS), heating wire, and a mini-channel test section with controlled temperature chamber. Pre-determined mass flow rates of methane and air were controlled by two digital mass flow controllers, and were fully mixed in a mixer before entering upstream to the small-scale channel test section, as shown in Fig. 1. The small-scale channels test section consisted of single horizontal quartz tube having inner tube diameter of 3.9, 3, 2 and 1 mm (wall thickness of 1 mm) respectively with a length of 600 mm. These tube diameters covered the dimensions from less than to greater than the quenching distance for premixed methane–air combustion at room temperature. The pressure difference

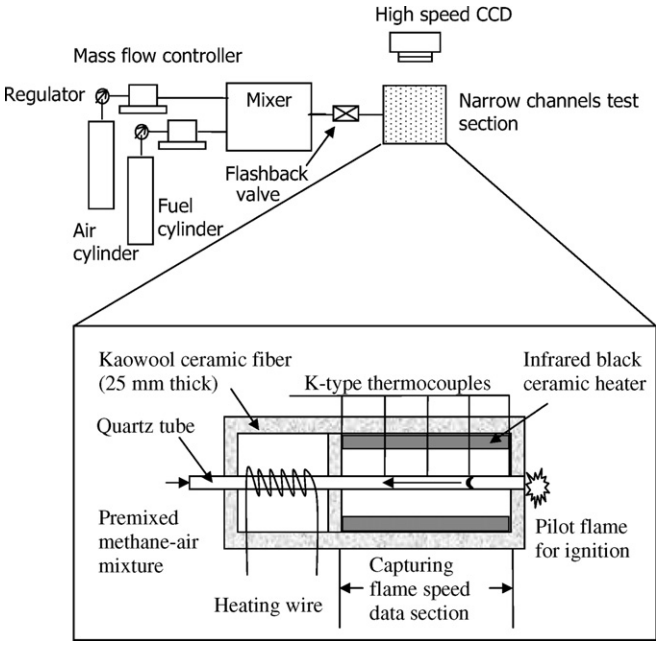

Fig. 1. Schematic diagram of the experimental setup.

between the inlet and outlet of the test section was measured by a pressure gauge. A controlled temperature chamber with different values of heat flux was used to preheat a section of the tube (245 mm long) where the flame speed was measured using a CCD camera system. The initial temperature of mixture and tube wall was controlled within ±5 °C. The controlled temperature chamber was built of high temperature Kaowool ceramic fibre (25 mm thick) which was further supported by high temperature bricks. Part of the Kaowool ceramic fibre was replaced by quartz plate for recording the flame speed. Temperature of the chamber was controlled by temperature controller (Barnant Company, Model 689-0015) connected to two infrared heaters and a K-type (RS 219-444) thermocouple with response time of 2 s. The preheated section of the tube was heated by infrared heaters placed above and under the tube (internal volume of preheated section, cm^3: $24.5 \times 10.5 \times 6$ ($L \times W \times H$). In order to ensure that the premixed gases reach the same temperature as the preheated section of the tube, heating wire was also used to heat up the premixed gases before entering to the preheated section of the tube. Five K-type thermocouples (RS 219-444) with 2 s response time were equally distributed (49 mm spacing) along the preheat section of tube to monitor the surface temperature of the tube. After confirming that the steady state had been reached, the premixed gases near the single open end of the tested tube were ignited by a pilot flame and the propagating flame speed was measured. The recorded images and elapse of time were processed in a PC to determine the flame speed. In the calculation, x denotes the longitudinal coordinate along the axis (from left to right). The premixed methane–air mixture flow velocity along the positive x direction relative to the wall is denoted by u_o. The flames propagate along the negative x direction with speed, u_f, relative to the tube wall. Absolute magnitude of flame speed, corresponding to flame movement against the mixture flow, is $u = u_o + u_f$. The reported flame speed was obtained by averaging the readings from three duplicated experiments. The accuracy of the propagating flame speed measurements was ±5%.

3.2. Preparation of catalysts

Molecular sieve type 13X in cylinder pellet (diameter: 3 mm, length: 5–7 mm) form (Nacalai Tesque, code: 233-36) was used to prepare catalyst in which the sodium ions were replaced by transition metal ions (Cu^{2+}) by the method of ion-exchange [26]. Several grams of 13X were held inside a tray and immersed in 100 ml of DI water over a period of 3 h under stirring (1000 rpm). Then, several drops of 2% HNO_3 were added to the solution until the pH was reduced to ~5. The purpose of adjustment of the pH value was to prevent the precipitation of hydroxide of Cu^{2+} ions. The calculated quantity of copper(II) sulphate salt (BDH, analytical grade) was dissolved in 100 ml of DI water and was added to the 13X-solution. The final concentration of the copper(II) sulphate solution (200 ml) was 0.1 M. The mixture was stirred (1000 rpm) for 24 h at 25 °C, then filtered and washed with DI water. Finally, the ion exchanged 13X was oven dried for 12 h at 120 °C. The exchanged process could be carried out again to obtain higher exchanged Cu^{2+} ions wt% in the zeolite 13X. For example, in sample Cu-13X-1 the number 1 means that the ion-exchange process was carried out once.

3.3. Characterization of catalysts

The chemical compositions of the catalyst was determined by a JEOL X-ray reflective fluorescence spectrometer (XRF, JSX 3201Z). Powder X-ray diffraction (XRD) pattern of the catalyst was obtained using a powder diffractometer (Philips PW 1830) equipped with a CuKα radiation. The accelerating voltage and current used were 40 kV and 20 mA, respectively. In order to study thermal stability of the catalyst, thermogravimetry (TG) in combination with differential thermal analysis (DTA) (TGA/DTA, Setaram 92-18) experiment was carried out. In the experiment, the sample was placed in a platinum holder and heated from 25 to 800 °C at a heating rate of 10 °C/min in air. Alpha alumina powder was used as a standard reference material for DTA. The pH value of the aqueous solution was measured by a Mettler-Toledo meter (MP 120).

4. Results and discussion

4.1. Analytical results

Activation energy asymptotics (AEA) is a powerful tool that has had stunning success in explaining a broad variety of low Mach number (β is in the range of 10–20) combustion phenomena [27]. The construction of asymptotic solutions is based on the jump condition derived in the limit of infinite β. AEA may be of questionable quantitative use if finite β is used to derive the jump condition. Regarding the choice of β in the AEA analysis, Buckmaster et al. [27] have commented that "no *a priori* argument can predict that 10^6 is large enough or that 1 is too small; a test based on experimental data is required to confirm the AEA analysis". In the current study, asymptotic solution was based on the jump condition derived in the limit of infinite β. In order to investigate the influence of preheat temperature on flame propagation and extinction feature of premixed methane–air flame in mini tubes, finite beta was used in the analysis. In the low Mach number flame, the β is of the magnitude of 10. For realistic value of the activation energy (e.g. $E = 124{,}650$ J/mol) and under the studied β conditions, the dimensionless reaction rates are very small (in the range of order of magnitude of 10^{-9} to 10^{-42}) in the preheat and the product zones which can be neglected. Thus, the asymptotic analysis could still be used to approximate the solution (influence of preheat temperature on flame propagation and extinction feature) in the current study. In the

following discussion, several parameters (preheat temperature, Zeldovich number β, dimensionless heat transfer coefficients and dimensionless tube radius) were varied to study their influences on the propagation of methane–air flame in the quartz tube. The mixture density at 300 K is $\rho = 1.774\ \text{kg/m}^3$; the specific heat at constant pressure, $c_p = 1005.7\ \text{kJ/kg K}$. The thermal diffusivity of gas phase, $\alpha = 2.22 \times 10^{-5}\ \text{m}^2/\text{s}$. The chemical heat release per unit mass of fuel is $3.8 \times 10^7\ \text{J/kg}$ and the activation energy of chemical reaction, $E = 1.2465 \times 10^5\ \text{J/mol}$. The reaction frequency factor of the chemical reaction, $B = 8.5 \times 10^8\ \text{s}^{-1}$ is so chosen that it yields 41 cm/s burning velocity at stoichiometric concentration. These parameters have been successfully used to simulate methane–air combustion [12,25]. For simplicity and illustrative purpose, the characteristics of flame propagation are examined for zero flow rate and the fuel concentration of $Y_{F0} = 0.0365$ is used which corresponds to the fundamental flammability limit of methane–air mixture at the initial temperature of 300 K [28].

4.1.1. Effects of preheat temperature and activation energy on Zeldovich number (β)

Table 1 shows the variation of the Zeldovich number under different preheat temperatures and activation energies. It is shown that keeping the activation energy unchanged, the Zeldovich number decreases with increasing preheat temperature. Keeping the preheat temperature unchanged, Zeldovich number increases with increasing activation energy. Fig. 2(a) shows the dependence of dimensionless flame speed on dimensionless heat transfer coefficient of the inner wall surface at $U_0 = 0$ and $R = 1.95$ mm and various Zeldovich numbers. In the nomenclature and Section 2, the dimensionless flame speed, U, was defined as $U_0 - U_f$, where $U_0 = u'_0/S_L$ and $U_f = u'_f/S_L$. Fig. 2(a) represents the condition $U_0 = 0$, thus, $U = -U_f = -u'_f/S_L$. S_L is the asymptotic value of the adiabatic planar burning velocity calculated in the limit $\beta \gg 1$, $S_L = \sqrt{2\beta^{-2}B\alpha Le}\exp(-T_a/2T_{ad})$. For clarity purpose, only the magnitude of U was reported in this paper. It is seen

Table 1
Variations of Zeldovich number with preheat temperature and activation energy

β	T_0, K	E, J/mol
3.2	1173	124,650
4.5	773	124,650
4.7	723	124,650
5.0	663	124,650
5.3	603	124,650
6.4	423	124,650
6.7	373	124,650
7.1	323	124,650
7.3	300	124,650
9.0	300	152,980
10.3	300	175,846
11.0	300	186,970
15.0	300	254,960

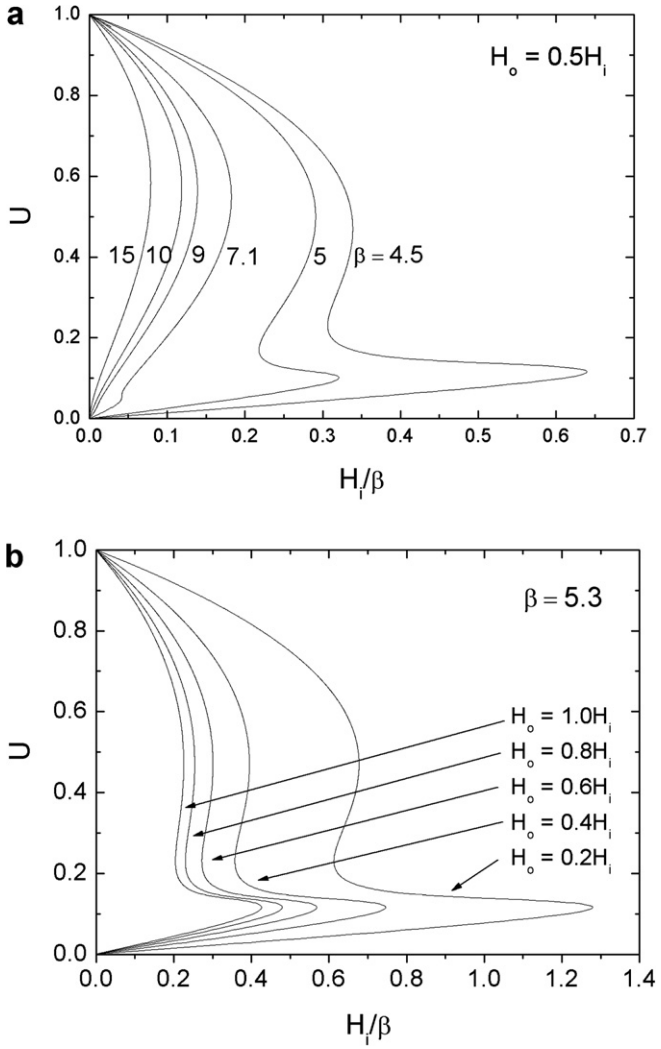

Fig. 2. (a) Dependence of normalized flame speed on dimensionless heat transfer coefficient for the inner wall surface at $U_0 = 0$ and $R = 1.95$ mm at various Zeldovich numbers; (b) dependence of normalized flame speed on dimensionless heat transfer coefficient for the inner wall surface at $U_0 = 0$ and $R = 1.95$ mm at various H_o.

that the flame behaves differently at different Zeldovich numbers. For $\beta \geqslant 9$, there exists only one steady state solution. The flame speed decreases with increasing dimensionless heat transfer coefficient. This is because of the increase in the wall heat loss. At a critical heat loss (at the turning point), flame extinguishes and no flame exists for larger heat loss. This extinction limit is caused by the wall cooling to the flame and is used to determine the quenching diameter [29]. For $\beta \leqslant 7.1$, there exists two steady state solutions of the flame speed, which is different from the result of $\beta \geqslant 9$. One is the traditional extinction limit which is termed the fast flame branch, while another extinction limit is a new flame branch which is termed the slow flame branch. With the decrease of the Zeldovich number, the fast flame extinction limit moves to the large heat transfer rate. The flame can be sustained at large heat loss, which indicates that the flammability limit is extended. The slow flame branch exists at very low flame speed, which is caused

by the external preheating to reduce the wall heat loss while keeping the activation energy constant. The increased wall temperature compensates the wall heat loss and sustains the flame. It is expected that influence of heat transfer from the burnt gas to the fresh gas by the wall also plays a role in sustaining the flame. The slow flame extinction limit moves to the large heat transfer rate with the decrease of the Zeldovich number. Further reducing the Zeldovich number, the slow flame extinction limit moves outside of the fast flame extinction limit and the turning point occurs far beyond the fast flame turning point. At $\beta = 7.1$, the slow flame branch can only exist at small heat loss. However, at $\beta \geqslant 5$, the flame can be held at very large heat loss which is even greater than the fast flame extinction limit. These two steady state solutions agree with the results of Ju and Xu [12] which support the findings at non-zero flow velocity. It is different from Ju and Xu [12] where the slow flame branch is caused by the weak flow velocity, and there is no slow flame branch at zero flow velocity. In our analysis, the slow flame limit is caused by external heating and heat recirculation, whereas in Ju and Xu [12] study, the slow flame limit is caused by heat recirculation of the wall from the burned gas region to the unburned gas via heat conduction in the wall. The results imply that at small-scale the flames can be sustained much beyond the traditional quenching diameter if a proper Zeldovich number is selected, which can be adjusted through different combination of the preheat temperature and the activation energy. With the concept of β on combustion in small scale, we could apply catalyst to reduce the activation energy of combustion in small scale or micro scale. The model also provides a way to understand the influence of catalysts on combustion in small scale or micro scale.

Fig. 2(b) shows the effects of H_0 on dimensionless flame speed versus dimensionless heat transfer coefficient of the inner wall surface at $U_0 = 0$ and $R = 1.95$ mm. It is seen that with the decrease of the dimensionless outer heat transfer coefficient, the flame extinction limit is extended to larger inner heat transfer rate. The results show qualitative agreement with the one-dimensional planar flames with volumetric heat losses [17]. Under the same dimensionless inner heat transfer coefficient, the flame speed increases with the decrease of the dimensionless outer heat transfer coefficient.

4.1.2. Effects of dimensionless heat transfer coefficient on normalized flame speed

Fig. 3 shows the dimensionless flame speed versus dimensionless tube radius at $U_0 = 0$ for various Zeldovich numbers. In the upper branch, the flame speed increases with increasing values of $\varepsilon^{-1}[R/\delta_T]$ and it approaches the planar adiabatic flame velocity. As the dimensionless radius decreases, the flame velocity decreases and at the quenching radius the curve turns into the lower branch which is unstable. The unstable branch goes asymptotically to zero as $\varepsilon^{-1}[R/\delta_T]$ is increased. At $\beta \leqslant 7.1$, the results are different from the traditional one. There are two stable solutions, the fast flame branch and the slow flame branch.

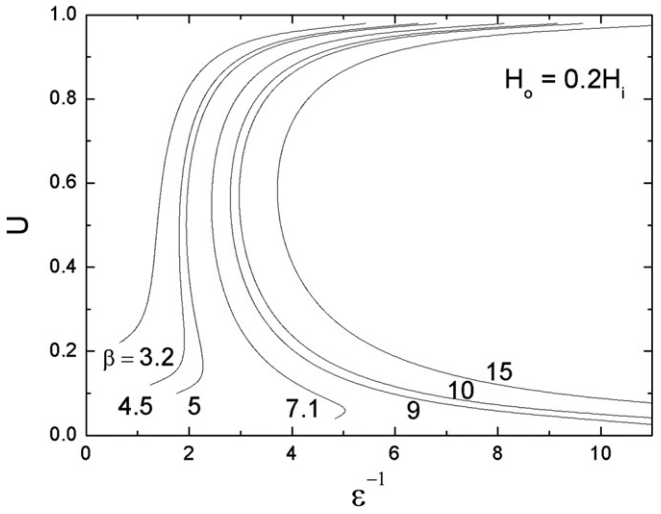

Fig. 3. Normalized flame speed versus dimensionless tube radius at $U_0 = 0$ for various Zeldovich numbers.

At $\beta \leqslant 5$, under the quenching diameter, the slow flame branch can still exist. Further reducing the Zeldovich number to $\beta = 3.2$, the restriction of quenching diameter is removed, and the flame velocity is monotonically increasing with the tube diameter. This implies that at sufficiently high initial temperature of mixture and tube wall, the gas phase flame can be sustained in micro-channels.

4.2. Experimental results

4.2.1. Without catalysts

4.2.1.1. Effects of the preheat temperature and the mixture volume flow rate on flame speed. In Section 3.1, absolute magnitude of flame speed, $u = u_0 + u_f$, was defined, where u_0 was the mixture flow velocity and u_f was the flame speed relative to the tube wall. In the current study, propagation of flame in narrow channels was investigated and flame propagated along the channels in all the experimental conditions. For clarity purpose, only the magnitude of flame speed, u, was reported in the following sections. For a quartz tube having an inner diameter of 3.9 mm, at 18 °C and atmospheric pressure, the flame can be sustained and propagated along the tube under different equivalence ratios (0.7–1). Fig. 4(a) shows that flame speed, u, generally increases with fuel concentration. Solid lines are the results of analytical model. This is because the change of the initial fuel concentration leads to the change of the flame temperature, and this affects the flame speed. Under the same preheat temperature (50 or 75 or 100 °C), it was observed that the flame speed increases and the flammability limit shifts toward the fuel lean direction when the mixture flow rate is decreased from 50 to 30 ml/min. This is because the decrease of the mixture flow velocity in a tube reduces the heat loss, thus a higher flame speed and an extended flammability limit were observed. As shown in Fig. 4(b), under the same mixture flow rates (50 or 40 or 30 ml/min), the flame speed increased and the flammability limits

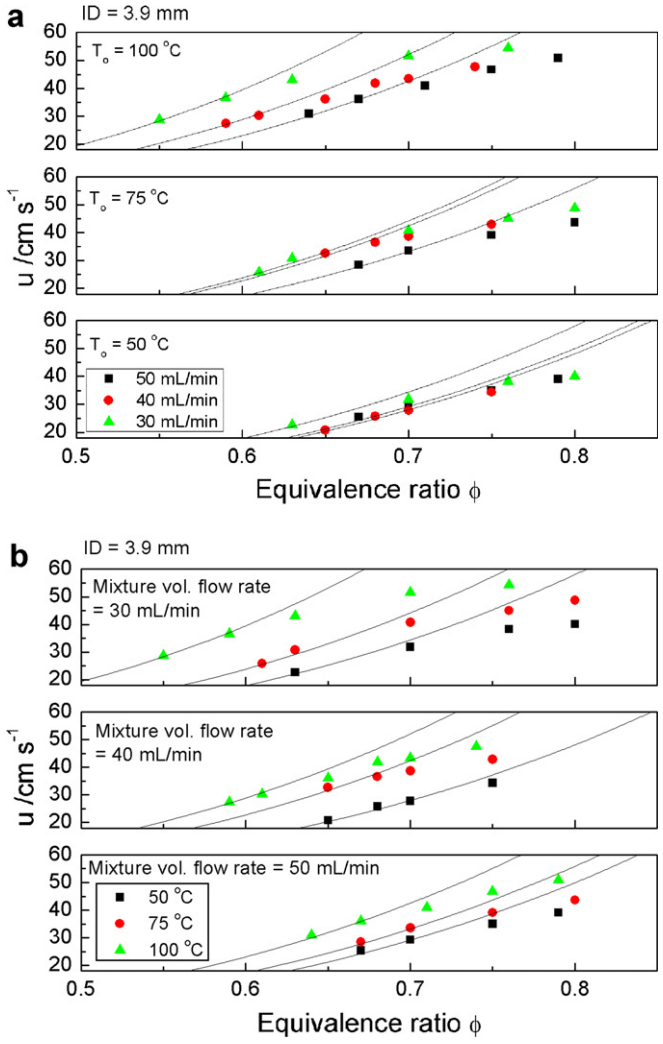

Fig. 4. Variation of propagating flame speeds with equivalence ratio for (a) different preheat temperatures under ambient pressure; (b) different mixture flow rates under ambient pressure. Lines are the results of analytical model.

shifted toward the fuel lean direction when the preheat temperature was increased from 50 to 100 °C. This is because increasing the preheat temperature leads to both the increase of the reaction temperature and the reduction in heat loss, thus a higher flame speed occurs under high preheat temperatures. For mixture volume flow rate of 30 ml/min, the flammability limit in the fuel lean branch is extended from an equivalence ratio of 0.63–0.55 when the preheat temperature is increased from 50 to 100 °C. The experimental results are in agreement with the analytical results.

In the work of Zamashchikov [8] (Fig. 3 of [8]), a low velocity regime was observed under small flame speed (the magnitude of which is smaller than 3 cm/s). It was due to preheating unburnt mixture through the wall of the tube by the burnt mixture. The experimental conditions such as quartz inner tube diameter of 4.9 mm, methane/air mixture of equivalence ratio of 1 and volume flow rate of 340–1000 ml/min were used in Ref. [8]. In the current study, influence of preheat temperature on flame propagation and extinction features of premixed methane/air flame in narrow channel was investigated. Experimental conditions such as quartz inner tube diameter of 3.9 mm, equivalence ratio of 0.5–0.8, preheat temperature of 50–100 °C and volume flow rate of 30–50 ml/min were used. In the current study, no low velocity regime was observed in the tested conditions. It may be because different experimental conditions were applied.

4.2.1.2. Effects of tube diameter. For a quartz tube having an inner diameter of 3 mm, a minimum preheat temperature of 150 °C is required to sustain a propagating flame along the preheated section of the tube. Fig. 5 shows the variation of propagating flame speeds with equivalence ratio for different mixture flow rates and preheat temperatures under ambient pressure. Solid lines are the results of analytical model. At preheat temperature $T_0 = 450$ °C, decrease of propagating flame speed is observed around equivalence ratio of 0.9 and 0.85 for a mixture flow rate of 50 ml/min, 40 ml/min and 30 ml/min. This observation may be explained using the comments by Popp and Baum [30]. It is suggested that when the wall temperature is between 127 °C and 327 °C, the fuel/air mixture cannot be considered inert and surface reactions (adsorption and desorption) have to be taken into account. At wall temperature of 327 °C, the CH_4 decomposition path and the chain-branching path decay by a factor of 2, whereas the methane recombination proceeds at almost the same rate as in the flame and this removes radicals from the flame very efficiently. In addition, there is an increase in the concentrations of H and OH radicals in the near-wall region which attributes to the higher rate of recombination reaction ($H + OH + M \rightarrow H_2O + M$) than in the free flame, thus the flame structure is changed. It is speculated that the decline of the flame speed may be due to the effect of

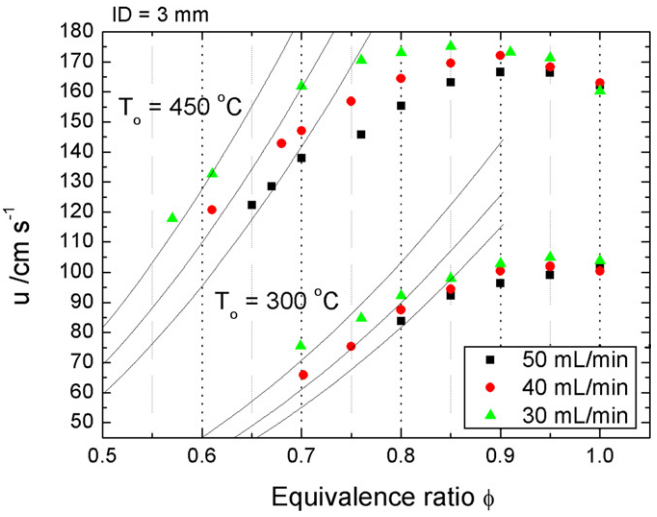

Fig. 5. Variation of propagating flame speeds with equivalence ratio for different preheat temperatures and mixture flow rates under ambient pressure. Lines are the results of analytical model.

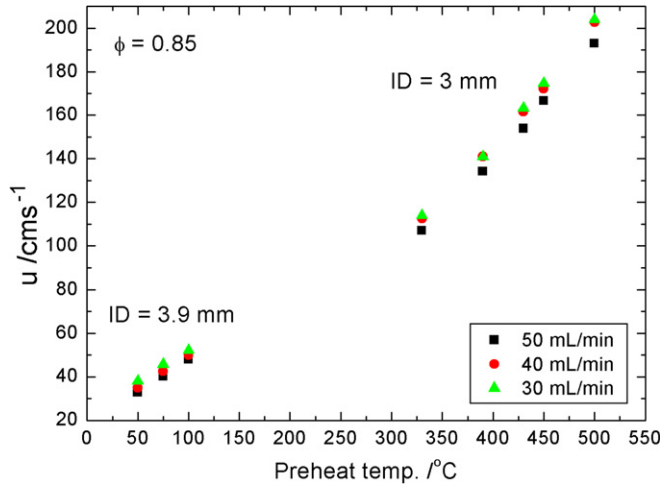

Fig. 6. Effect of preheat temperature on flame speed under ambient pressure.

reduced rates of the CH_4 decomposition and the chain-branching, as well as the increased rate of recombination reaction of H and OH radicals in the near-wall region. It is noticed that the analytical model is only good at the fuel lean branch. This may be due to the two-dimensional curve flame structure and the simplified one-step irreversible reaction step used in the model which neglects the recombination reaction of H and OH radicals in the near-wall region under high initial temperature of tube wall. Based on the study by Popp and Baum [30], it is expected that higher activation energy should be selected to model the flame speed in the equivalence ratio of 0.85–1.0. However, the proper choice of the activation energy was not investigated in the present study. Fig. 6 shows the effects of preheat temperature on flame speed in different tube diameters under different mixture flow rates. The results confirm that the flame speed increases with preheat temperature under the same mixture flow rate, and the flame speed increases with decreasing the mixture flow rate under the same preheat temperature.

For a quartz tube of inner diameter of 2 mm, a minimum preheat temperature of 900 °C was required to ignite a propagating flame along the preheated section of the tube. The results obtained from this experiment indicated that when the tube diameter was further reduced, a very high preheat temperature was required to sustain a propagating flame in the tube. However, from thermal management point of view, implementing micro-combustion devices at very high temperature is not practical. This leads to the usage of catalyst in micro-combustors to reduce the operational temperature and to extend the flammability limits as will be discussed in the next section.

4.3. With catalysts

4.3.1. Characterization of the catalyst

Chemical composition of the original zeolite 13X, Cu-13X-1 and Cu-13X-2 is shown in Table 2. It is shown that

Table 2
Chemical composition of the zeolite 13X, Cu-13X samples by XRF measurement

wt%	Zeolite 13X	Cu-13X-1	Cu-13X-2
Si	53.87	40.76	36.36
Al	29.82	26.21	23.95
Na	13.28	6.27	4.83
Cu	0.00	24.24	30.78
K	0.92	0.58	0.47
Ca	0.18	0.14	0.11
Fe	1.04	0.69	0.62

the wt% of Cu loading is increased with the times of ion-exchanged process. Fig. 7(a) shows the XRD patterns of the samples where zeolite 13X, Cu-13X-1 and Cu-13X-2 are identified as single phase crystals (JCPDS card 39-0218). After the ion-exchange processes, the crystallinity of the samples was reduced. These variations may be due to the differences in the chemical composition of the samples after the ion-exchange processes. However, the *d*-spacings of the Cu-13X-1 and the Cu-13X-2 samples were the same as the zeolite 13X showing that the crystal structure of the samples was not altered during the ion-exchange treatment. In addition, no characteristic peaks of CuO

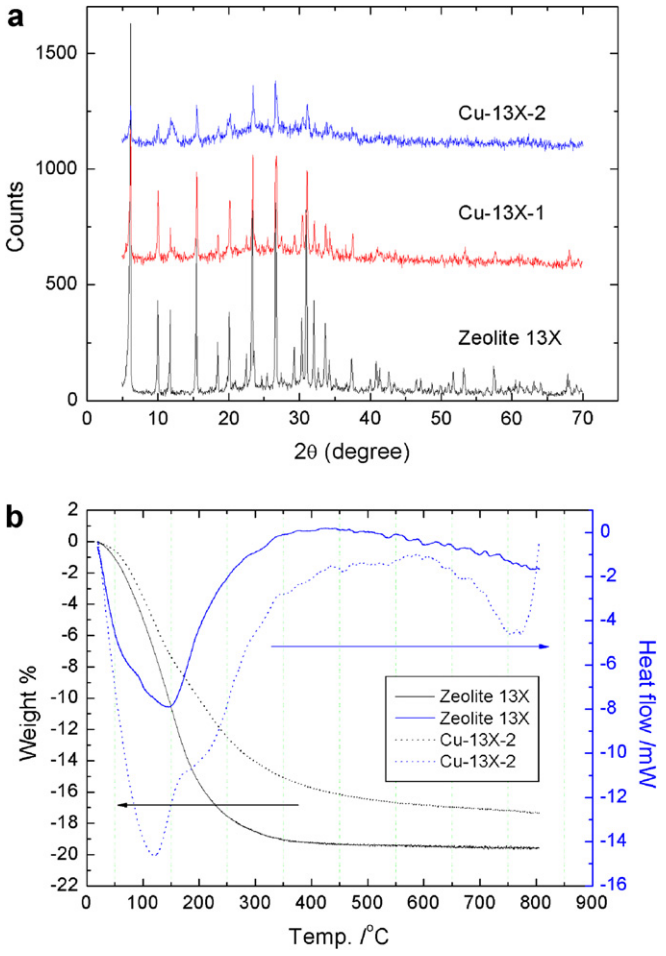

Fig. 7. (a) The XRD pattern of the catalysts; (b) the TG–DTA curves of the zeolite 13X and Cu-13X-2.

($2\theta = 35.4°$, 38.8°) were found in the XRD patterns suggesting that no bulk metal oxides existed in the prepared samples.

The TG–DTA curves of the zeolite 13X and Cu-13X-2 are shown in Fig. 7(b). In TG curves, there were two major weight loss steps. The first below 150 °C was due to the loss of physically adsorbed water, and the second, between 150 and 400 °C, was due to the decomposition of organic substances (the binder used in zeolite 13X). After 400 °C, no significant weight loss was found, indicating the complete removal of the organic substances. In the DTA curves, the first endothermic peaks center around 100–150 °C corresponding to the loss of water. For Cu-13X-2 sample, another endothermic peak centers around 750 °C corresponding to the collapse of zeolite 13X framework. From the TG–DTA results, it is deduced that a relatively high thermal stability of the Cu^{2+} ions exchanged sample can be obtained.

4.3.2. Influence of Cu-13X catalyst on flame speed

The catalyst was located 80 mm downstream of the preheated section of the tube. Without the catalyst, it was observed that flame could not be propagated in the inner diameter of 3 mm tube under certain fuel lean conditions. With the catalyst, the lean flammability limit was slightly extended towards the fuel lean direction. At 450 °C, the lean flammability limit was extended from 0.65 to 0.63, 0.61 to 0.58 and 0.57 to 0.54 under volume flow rate of 50, 40 and 30 ml/min, respectively. Fig. 8 shows the magnitude of propagating flame speed in an inner diameter of 3 mm quartz tube under different preheat temperatures with and without the addition of catalyst (0.0551 g). With the catalyst, the flame speeds generally were faster under different mixture flow rates than that without catalyst. The increase in flame speed may be due to the partial conversion of methane into hydrogen which enhances the flame speed. However, there was no clear relationship observed in the percent increase in flame speed under different mixture flow rates. The results imply that the increase in flame speed under the addition of catalyst can lead to the propagation of flame in a narrower channel under the same preheat temperature. It is because flame speed is an indication of the reactivity and exothermicity of a mixture. The higher the flame speed the lower the quenching diameter.

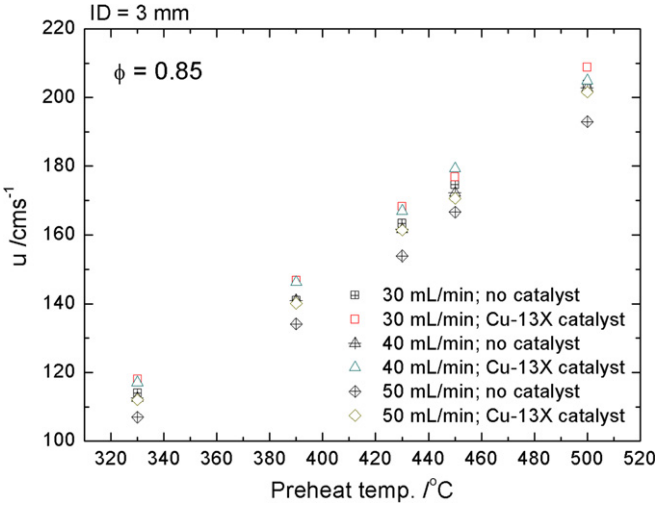

Fig. 8. Influence of catalyst on the propagating flame speed in quartz tube under different preheat temperatures and at ambient pressure.

5. Conclusions

Based on activation energy asymptotics approach, an analytical solution is obtained for flame propagation and extinction in mini-channels. The results show that high preheat temperature can effectively suppress flame quenching, leading to multiple flame regimes and extinction limits. The extinction limit shifts toward the fuel lean direction and the flame speed increases with preheat temperature. The occurrence of stable solution in the slow flame branch extends the flammability limit, leading to possible flame propagation in mini-channels. With the decrease of the outer wall heat loss, the flame speed increases and the extinction limit is extended. The analytical model provides some insights into sustaining propagating flame in micro-channels but it only seems to be good at predicting flame speed near the fuel lean branch. Experimental results show that minimum preheat temperatures for the occurrence of propagating premixed methane–air flame were 18, 150 and 900 °C for quartz tubes of inner diameters of 3.9, 3 and 2 mm (wall thickness of 1 mm), respectively. Generally, the experimental results are in qualitative agreement with the analytical results. Decrease of propagating flame speed was observed before stoichiometric equivalence ratio under high initial temperature of mixture and tube wall. In order to develop micro-power devices, catalyst assisted combustion should be adopted which can eliminate the problems of thermal management of the devices and reduce the activation energy for the combustion reaction, thus a lower preheat temperature can be used to sustain combustion in micro-channels. Experiments related to stabilizing combustion zone in mini quartz tubes under the addition of catalyst deserve further investigation. The results of this study will be useful to design of micro-combustors.

Acknowledgements

This project was supported by the Hong Kong Research Grant Council via project number HKUST6188/03E, and was partially supported by the National Natural Science Foundation of China through contract number 50536010.

References

[1] A.C. Fernandez-Pello, Micropower generation using combustion: issues and approaches, Proc. Combust. Inst. 29 (2003) 883–899.
[2] A.H. Epstein, S.D. Senturia, Macro power from micro machinery, Science 276 (5316) (1997) 1211.

[3] K. Fu, A.J. Knobloch, B.A. Cooley, D.C. Walther, D. Liepmann, K. Miyasaka, A.C. Fernandez-Pello, Microscale combustion research for applications to MEMS rotary IC engine, in: Proceedings of the National Heat Transfer Conference, Ananheim, CA, 2001, pp. 613–618.
[4] H.T. Aichlmayr, D.B. Kittelson, M.R. Zachariah, Micro-HCCI combustion: experimental characterization and development of a detailed chemical kinetic model with coupled piston motion, Combust. Flame 135 (3) (2003) 227–248.
[5] F. Weinberg, Optimizing heat recirculating combustion systems for thermoelectric converters, Combust. Flame 138 (4) (2004) 401–403.
[6] C. Zhang, K. Najafi, L.P. Bernal, P.D. Washabaugh, A micromachined combustor and its application to micro thermoelectric power generation, in: American Society of Mechanical Engineers, Micro-Electromechanical Systems Division Publication (MEMS), New Orleans, LO, 2002, pp. 1–6.
[7] W.M. Yang, S.K. Chou, C. Shu, H. Xue, Z.W. Lil, Development of a prototype micro-thermophotovoltaic power generator, J. Phys. D–Appl. Phys. 37 (7) (2004) 1017–1020.
[8] V.V. Zamashchikov, Experimental investigation of gas combustion regimes in narrow tubes, Combust. Flame 108 (3) (1997) 357–359.
[9] V.V. Zamashchikov, S.S. Minaev, Limits of flame propagation in a narrow channel with gas filtration, Combust. Explo. Shock Waves 37 (1) (2001) 21–26.
[10] V.V. Zamashchikov, An investigation of gas combustion in a narrow tube, Combust. Sci. Technol. 166 (2001) 1–14.
[11] V.V. Zamashchikov, Some features of gas-flame propagation in narrow tubes, Combust. Explo. Shock Waves 40 (5) (2004) 545–552.
[12] Y.G. Ju, B. Xu, Theoretical and experimental studies on mesoscale flame propagation and extinction, Proc. Combust. Inst. 30 (2005) 2445–2453.
[13] K. Maruta, T. Kataoka, N.I. Kim, S. Minaev, R. Fursenko, Characteristics of combustion in a narrow channel with a temperature gradient, Proc. Combust. Inst. 30 (2005) 2429–2436.
[14] K. Maruta, J.K. Parc, K.C. Oh, T. Fujimori, S.S. Minaev, R.V. Fursenko, Characteristics of microscale combustion in a narrow heated channel, Combust. Explo. Shock Waves 40 (5) (2004) 516–523.
[15] I. Glassman, Combustion, 3rd ed., Academic Press, San Diego, 1996.
[16] J. Daou, M. Matalon, Flame propagation in Poiseuille flow under adiabatic conditions, Combust. Flame 124 (3) (2001) 337–349.
[17] J. Daou, M. Matalon, Influence of conductive heat-losses on the propagation of premixed flames in channels, Combust. Flame 128 (4) (2002) 321–339.
[18] J. Daou, J. Dold, M. Matalon, The thick flame asymptotic limit and Damkohler's hypothesis, Combust. Theory Model. 6 (1) (2002) 141–153.
[19] V.V. Zamashchikov, Combustion of gases in thin-walled small diameter tubes, Combust. Explo. Shock Waves 31 (1) (1995) 20–22.
[20] J.M. Ahn, C. Eastwood, L. Sitzki, P.D. Ronney, Gas-phase and catalytic combustion in heat-recirculating burners, Proc. Combust. Inst. 30 (2005) 2463–2472.
[21] P. Forzatti, G. Groppi, Catalytic combustion for the production of energy, Catal. Today 54 (1) (1999) 165–180.
[22] R. Rudham, M.K. Sanders, Catalytic properties of zeolite-X containing transition-metal ions. 2. Methane oxidation, J. Catalysis 27 (2) (1972) 287–292.
[23] N.V. Nekrasov, A.A. Slinkin, A.V. Kucherov, G.O. Bragina, E.A. Katsman, S.L. Kiperman, Kinetics of the complete oxidation of methane over the CuZSM-5 catalyst, Kinetics Catal. 38 (1) (1997) 77–80.
[24] J. Chomiak, Combustion: A Study in Theory, Fact and Application, 1st ed., Abacus Press, New York, 1990.
[25] T. Takeno, K. Sato, Excess enthalpy flame theory, Combust. Sci. Technol. 20 (1–2) (1979) 73–84.
[26] R. Rudham, M.K. Sanders, in: P. Hepple (Ed.), Chemisorption and Catalysis, Institute of Petroleum, London, 1971, pp. 58–71.
[27] J. Buckmaster, M. Short, D.S. Stewart, The use of activation energy asymptotics in detonation theory, Phys. Fluids 10 (11) (1998) 3027–3030, with comment on Multidimensional stability analysis of overdriven gaseous detonations, Phys. Fluids (9) (1997) 3764.
[28] Y.G. Ju, C.W. Choi, An analysis of sub-limit flame dynamics using opposite propagating flames in mesoscale channels, Combust. Flame 133 (4) (2003) 483–493.
[29] B. Lewis, G. von Elbe, Combustion, Flames, and Explosions of Gases, third ed., Academic Press, Orlando, 1987.
[30] P. Popp, M. Baum, Analysis of wall heat fluxes, reaction mechanisms, and unburnt hydrocarbons during the head-on quenching of a laminar methane flame, Combust. Flame 108 (3) (1997) 327–348.